

On the hiatus in the acceleration of tropical upwelling since the beginning of the 21st century

J. Aschmann¹, J. P. Burrows¹, C. Gebhardt¹, A. Rozanov¹, R. Hommel¹, M. Weber¹, and A. M. Thompson²

¹Institute of Environmental Physics, University of Bremen, Bremen, Germany

²NASA/Goddard Space Flight Center, Greenbelt, MD, USA

Abstract. Chemistry-climate models predict an acceleration of the upwelling branch of the Brewer-Dobson circulation as a consequence of increasing global surface temperatures, resulting from elevated levels of atmospheric greenhouse gases. The observed decrease of ozone in the tropical lower stratosphere during the last decades of the 20th century is consistent with the anticipated acceleration of upwelling. However, more recent satellite observations of ozone reveal that this decrease has unexpectedly stopped in the first decade of the 21st century, challenging the implicit assumption of a continuous acceleration of tropical upwelling. In this study we use three decades of chemistry-transport-model simulations (1980–2013) to investigate this phenomenon and resolve this apparent contradiction. Our model reproduces the observed tropical lower stratosphere ozone record, showing a significant decrease in the early period followed by a statistically robust trend-change after 2002. We demonstrate that this trend-change is correlated with structural changes in the vertical transport, represented in the model by diabatic heating rates taken from the reanalysis product Era-Interim. These changes lead to a hiatus in the acceleration of tropical upwelling between 70–30 hPa during the last decade, which appears to be the primary cause for the observed trend-change in ozone.

1 Introduction

The issue of whether the large-scale Brewer-Dobson Circulation (BDC) has strengthened in the recent past, as a result of anthropogenic activity, has been raised (Oman et al., 2009; Butchart et al., 2010; Randel and Jensen, 2013). Recent chemistry-climate model (CCM) simulations predict an increase of resolved wave activity and orographic gravity

wave drag resulting from increasing sea surface temperatures (SST; Garcia and Randel, 2008; Oman et al., 2009; Waugh et al., 2009; Butchart et al., 2010; Garny et al., 2011). This strengthens the upwelling branch of the BDC, commonly referred to as the tropical upwelling. In comparison, the behaviour of the observations available since about 1980 is ambiguous. The long-term cooling of the tropical lower stratosphere (LS, about 17–21 km; Thompson and Solomon, 2005; Young et al., 2012) and the observed weakening of the stratospheric quasi-biennial oscillation (QBO; Kawatani and Hamilton, 2013) are consistent with the predicted increase of upwelling. On the other hand, the mean residence time of air parcels in the stratosphere (age of air) inferred from sulfur hexafluoride (SF₆) measurements is inconsistent with an overall acceleration of the BDC (Engel et al., 2009; Stiller et al., 2012). Age of air changes indicate no significant changes or even deceleration of the vertical transport in the middle stratosphere. To reconcile the observed discrepancies it has been argued that the individual branches of the BDC are evolving differently, i.e. an increase of tropical upwelling does not necessarily imply an acceleration of the overall circulation (Bönisch et al., 2011; Diallo et al., 2012; Lin and Fu, 2013).

Ozone (O₃) is a sensitive proxy for vertical transport in the tropical LS (Randel et al., 2006; Waugh et al., 2009; Randel and Thompson, 2011; Polvani and Solomon, 2012). Its local mixing ratio is considered to result from a stationary state involving production by oxygen (O₂) photo-dissociation and a steady influx of O₃-poor tropospheric air from below (Avalone and Prather, 1996; Waugh et al., 2009; Meul et al., 2014). Meridional mixing from higher latitudes is another factor that contributes to the seasonality in the O₃ mixing ratios (Konopka et al., 2009; Ploeger et al., 2012; Abalos et al., 2013), with the largest impact during boreal summer directly above the tropopause (≈ 380 K/17 km). Several studies have reported a negative trend of O₃ in the tropical LS in the range of -(3–6) % per decade from about 1985 onwards, consistent

Correspondence to: J. Aschmann
(jan.aschmann@iup.physik.uni-bremen.de)

with the CCM predicted increase of tropical upwelling (e.g., Randel and Thompson, 2011; Sioris et al., 2014; Bourassa et al., 2014). In contrast, more recent O₃ observations from various satellite instruments indicate no statistically significant decrease of LS O₃ since the beginning of the 21st century (Kyrölä et al., 2013; Eckert et al., 2014; Gebhardt et al., 2014).

Stimulated by the need to explain the unusual linear trends revealed from the vertical profile of O₃ retrieved from SCIAMACHY¹ we use three decades of O₃ observations and simulations to investigate this phenomenon. Section 2 describes the observations, model and regression analysis used in this study. The results are discussed in Sect. 3.

2 Data and analysis

2.1 Observations

For a quantitative analysis of tropical upwelling, we use combined O₃ observations from satellite instruments and sondes. The earlier decades (1985–2005) are covered by the ERBS/SAGE II instrument (McCormick et al., 1989), providing O₃ profiles based on solar occultation measurements. Due to its viewing geometry, the vertical resolution of the profiles is high (1 km, range 15–50 km), although the horizontal sampling is relatively sparse (global coverage in 1 month). Here we use version 7.0 of the data (Damadeo et al., 2013), screened for cloud and aerosol contaminated profiles as suggested by Wang et al. (2002). Two years of data after June 1991 have been omitted due to contamination by the eruption of Mt. Pinatubo. For the last decade (2002–2012), we use O₃ observations from ENVISAT/SCIAMACHY (Burrows et al., 1995) based on limb geometry (retrieval version 2.9; Sonkaew et al., 2009). The vertical resolution is about 3–4 km over an altitude range of 10–75 km; global coverage is achieved every 6 days. Data from both instruments has been binned into monthly samples on a uniform horizontal and vertical grid (15°lon. × 5°lat. × 1 km). To minimise sampling issues and taking into account the differences in horizontal and vertical resolution of the instruments, any further analysis is based on partial columns of O₃ between 17–21 km and 20°N–20°S, similar to the approach of Randel and Thompson (2011).

The satellite data is augmented by an ensemble of tropical sonde measurements from the Southern Hemisphere Additional Ozonesondes network (SHADOZ; 1998–2013; Thompson et al., 2003, 2012). We use 10 sites located in the tropics with long and continuous records. The selected stations along with their temporal coverage and mean value are listed in Table 1. Typically there are 2–4 observations per month for each SHADOZ station, which provide O₃ profiles

¹First reported at the Quadrennial Ozone Symposium 2012 Toronto, August 27–31 2012 and published in Gebhardt et al. (2014)

in a considerably higher vertical resolution (50–100 m) compared to the satellite instruments. As there is a high degree of longitudinal symmetry in the stratospheric ozone profiles (Thompson et al., 2003), we average the individual records to obtain a representative mean for the tropics.

2.2 Model

To obtain a consistent timeseries of LS O₃ of the last decades for direct comparison with observations, we conducted a 33-year simulation with the Bremen three-dimensional chemistry-transport-model (B3DCTM; Sinnhuber et al., 2003; Aschmann et al., 2009; Aschmann and Sinnhuber, 2013). The current version of the model has a horizontal resolution of 3.75°lon. × 2.5°lat. and covers the vertical domain from the surface up to approximately 55 km using a hybrid $\sigma - \theta$ coordinate system (e.g., Chipperfield, 2006). The vertical resolution in the tropical LS is about 600 m. The model is driven by 6-hourly input of European Centre for Medium-range Weather Forecast (ECMWF) Era-Interim (EI; Dee et al., 2011) reanalysis data. Vertical transport in the purely isentropic domain (above ≈16 km in the tropics) is prescribed by EI all-sky heating rates. The B3DCTM incorporates a comprehensive chemistry scheme originally based on the chemistry part of the SLIMCAT model (Chipperfield, 1999), covering all relevant photochemical reactions for stratospheric O₃ chemistry. Reaction rates and absorption cross sections are taken from the Jet Propulsion Laboratory recommendations (Sander et al., 2011). Injection of ozone-depleting substances (ODS) is prescribed according to WMO scenario A1 (World Meteorological Organization, 2011). To avoid initialisation artefacts, the model has been run with replicated input data to reach steady state before starting the actual integration from January 1979 to October 2013.

2.3 Regression

The multivariate regression analysis used throughout this study is based on Reinsel et al. (2002) with Y_t as the monthly mean variable to be fitted:

$$Y_t = \mu + S_t + \omega_1 X_{1t} + \omega_2 X_{2t} + QBO_t + ENSO_t + SC_t + N_t \quad (1)$$

$$t = 1, \dots, T$$

where μ is the baseline constant, S_t a seasonal component, $\omega_{1,2}$ are the trend coefficients with $X_{1,2t}$ as trend functions:

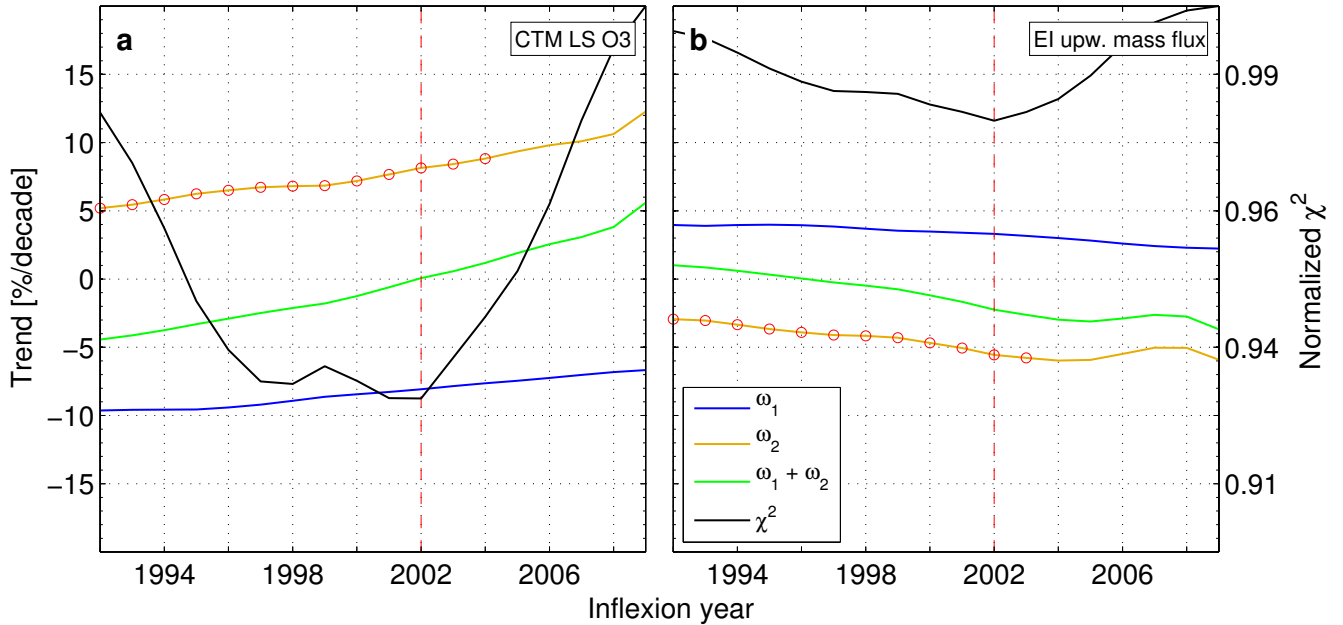
$$X_{1t} = t/12 \quad (2)$$

$$X_{2t} = \begin{cases} 0 & 0 < t \leq T_0 \\ (t - T_0)/12 & T_0 < t \leq T \end{cases} \quad (3)$$

Note that in contrast to most previous studies, which examined LS O₃ (e.g., Randel and Thompson, 2011; Sioris et al., 2014), our regression model uses two linear components to take into account a possible change of trend at a given point

Table 1. Geolocation, temporal coverage and average LS O₃ column of utilised SHADOZ sites.

Name	Location		Coverage	Average [DU]
Ascension Is.	14.4°W	8.0°S	01/1998 – 08/2010	28.76
Costa Rica	84.0°W	9.9°N	07/2005 – 12/2012	30.66
Hilo	155.0°W	19.4°N	01/1998 – 02/2013	36.97
Watakosek-Java	112.6°E	7.5°S	01/1998 – 06/2013	27.06
Kuala Lumpur	101.7°E	2.7°N	01/1998 – 12/2011	30.26
Nairobi	36.8°E	1.3°S	01/1998 – 06/2013	30.66
Natal	35.3°W	5.5°S	01/1998 – 05/2011	29.74
Paramaribo	55.2°W	5.8°N	09/1999 – 12/2011	31.53
Samoa	170.6°W	14.2°S	01/1998 – 12/2012	30.91
San Cristobal	89.6°W	0.9°S	03/1998 – 10/2008	29.26

**Fig. 1.** The dependence of the linear fit parameters ω_1 , ω_2 and ω ($\omega_1 + \omega_2$) on the inflexion year T_0 is shown for the regression of modelled tropical LS O₃ column (a) and EI upward mass flux at 70 hPa (b). Red circles denote the years where the trend-change (ω_2) exceeds the 95% confidence threshold. The black lines are the normalised χ^2 values of the fit residuals.

in time. ω_1 is the linear trend up to a specified inflexion date T_0 . After T_0 , the new linear trend ω comprises the sum of the earlier trend ω_1 and the trend-change component ω_2 . The additional regression terms are QBO_t for QBO, $ENSO_t$ for the El Niño Southern Oscillation (ENSO) and SC_t for solar cycle. The QBO proxy consists of the QBO.U30 and QBO.U50 (zonal wind 30/50 hPa) from the NOAA Climate Prediction Center², the ENSO proxy is represented by the Multivariate ENSO Index (MEI) from the NOAA Earth System Research Laboratory³ (Wolter and Timlin, 2011) lagged by two months and the solar cycle by the Bremen composite Mg II

index⁴ (Snow et al., 2014). Finally, N_t represents the unexplained noise.

Assuming first order autocorrelation noise (AR(1) model), as commonly used in the regression of O₃ timeseries (e.g., Reinsel et al., 2002; Jones et al., 2009; Sioris et al., 2014), the corresponding standard deviations for the trend components

²www.cpc.ncep.noaa.gov/data/indices/

³www.esrl.noaa.gov/psd/enso/mei/

⁴www.iup.uni-bremen.de/gome/solar/MgII.composite.dat

are given by

$$\sigma_{\omega_1} \approx \frac{\sigma_N}{n^{3/2}} \sqrt{\frac{1+\phi}{1-\phi}} \quad (4)$$

$$\sigma_{\omega_2} \approx \frac{\sigma_N}{2} \sqrt{\frac{1+\phi}{1-\phi}} \left(\frac{n}{n_0 n_1} \right)^{3/2} \quad (5)$$

$$\sigma_{\omega} \approx \frac{\sigma_N}{n_1^{3/2}} \sqrt{\frac{1+\phi}{1-\phi}} \sqrt{\frac{n_0+4n_1}{4n}} \quad (6)$$

where σ_N is the standard deviation of the fit residuals, n_0 , n_1 are the numbers of years of data before and after the trend-change, respectively, with $n = n_0 + n_1$. ϕ represents the autocorrelation of the residuals with a time lag of 1 month.

The choice of the inflexion year T_0 is a free parameter found in the regression analysis. Figure 1 illustrates the impact of the choice of T_0 on the regression of modelled LS O_3 columns and EI upward mass flux (as discussed below in Sect. 3). A 2σ -significant trend-change (ω_2) is obtained for a range of possible inflexion years (marked by red circles). We therefore use a χ^2 fit based on the regression residuals, similar to the approach described by Jones et al. (2009), to identify the most probable inflexion year. We find a clear minimum in the χ^2 values close to 2002 and consequently select this year as the turning point in the trend analysis.

3 Results and Discussion

3.1 Lower stratosphere ozone column

Figure 2 presents tropical LS O_3 column anomalies (20°N – 20°S , 17–21 km) from measurements and the simulation. The agreement between model and observations is good, except for a small high-bias relative to the earlier SAGE II data (1985–1990) of approximately 1 DU: correlation coefficients are 0.65 between modelled and observed datasets.

A decline of O_3 is evident in the tropical LS during the first two decades (1980–2002), both in the observed and modelled timeseries. This is consistent with an increase of tropical upwelling during this period. However, this trend vanishes in the third decade (2002–2013). Figures 3a and b illustrate the results from the regression analysis of the modelled timeseries showing the fit function and the corresponding residuals, respectively. The linear trend amounts to -8.1 ± 0.9 % per decade (ω_1) in the pre-2002 period and 0.1 ± 3.3 % per decade (ω) for the remaining years. The resulting trend-change of 8.2 % per decade (ω_2) is statistically significant within the 95% confidence interval (i.e. $\omega_2 > 2\sigma_{\omega}$).

To apply our analysis to the observational data we merge the available datasets (SAGE II–SCIAMACHY; SAGE II–SHADOZ) by joining the two individual timeseries and average the overlap period. In case of SAGE II–SHADOZ, this method has been applied before by Randel and Thompson (2011) who found excellent agreement between SHADOZ

and SAGE II in tropical LS O_3 , despite the sparse horizontal sampling provided by the sondes. SAGE II and SCIAMACHY show similarly good agreement in this area, with a correlation of 0.82 and an average bias of 0.5 DU (< 2 %) during the overlap period. Considering the good agreement between the observations (Fig. 3), it is reasonable to combine them into a continuous timeseries. When we apply the regression to the combined SAGE II–SCIAMACHY timeseries, we calculate a trend of -3.9 ± 0.5 % per decade (ω_1) for the pre-2002 period, consistent with the range of $-(3\text{--}6)$ % per decade given by earlier studies (Fig. 3c, d; Randel and Thompson, 2011; Sioris et al., 2014; Bourassa et al., 2014). However, this value is smaller than the pre-2002 trend determined from our CTM simulations. Considering the good agreement between observations and model after the Mt. Pinatubo data gap (1991–1994), the discrepancy must be mainly caused by the model high-bias compared to the early SAGE-II measurements. The origin of this bias is not entirely clear. Assuming that the SAGE II record is consistent before and after the Mt. Pinatubo eruption, the bias is possibly explained by a spin-up effect of the model stemming from the usage of replicated input data for the initialisation phase (Sect. 2.2). Another point could be the overestimation of the vertical transport velocity based on diabatic heating rates in the EI dataset (Ploeger et al., 2012; Diallo et al., 2012), which is discussed in more detail in Sect. 3.2. After 2002, the agreement between model and observations improves considerably and the trend is 0.5 ± 1.5 % per decade (ω), yielding a statistically significant trend-change of 4.4 % per decade (ω_2) for the SAGE II–SCIAMACHY dataset. We obtain similar values (-3.6 ± 0.5 , 0.4 ± 1.4 % per decade for ω_1 , ω) if we use the SHADOZ data instead of SCIAMACHY in the combined dataset (Fig. 3e, f). Consequently, both observational and model data show that the decrease of LS O_3 effectively stopped around 2002 and there has been no significant change afterwards. This is in qualitative agreement with those studies, which focus solely on the most recent observational record of O_3 , although the differences in utilised regression models and timeseries length make a direct comparison difficult. Gebhardt et al. (2014) compared several satellite instruments and report consistently positive trends of tropical O_3 between 17–21 km, ranging from about 2 (OSIRIS), 4 (SCIAMACHY) up to 14 % per decade (MLS), covering the years 2004–2012. Eckert et al. (2014) find a slightly positive trend of 0–1 % per decade in the same region in MIPAS observations (2002–2012). In summary, despite the considerable spread in the determined trends all instruments described above show no further decrease of tropical LS O_3 during the last decade. This agreement justifies our confidence that this phenomenon is not an instrumental or retrieval artefact.

Local chemical effects can be largely ruled out as explanation for the detected trend-change of LS O_3 . As stated above, O_3 abundance in the tropical LS is mainly determined by vertical transport and O_2 photolysis (Avallone and Prather,

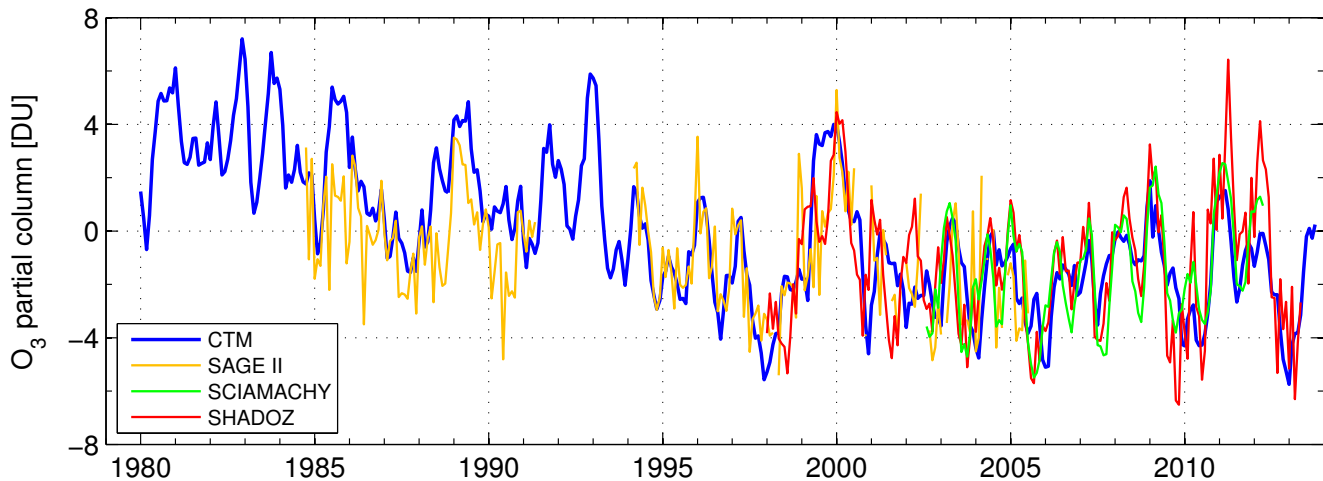


Fig. 2. Observed and simulated tropical (20°N – 20°S) LS O_3 partial columns (17–21 km). Anomalies are deviations from the modelled 1980–2013 averages.

1996; Waugh et al., 2009; Meul et al., 2014). O_3 -destroying catalytic species are scarce in the tropical LS, therefore the phase-out of ODS, and the associated recovery (e.g., World Meteorological Organization, 2011), has no direct impact on O_3 concentrations in this region. To verify this assumption, we have conducted a sensitivity simulation with identical setup but with ODS emissions fixed to the values of 1980 (not shown here). In contrast to mid and high latitudes, the O_3 mixing ratios in the tropical LS show little difference to the standard simulation ($<2\%$) and we calculate very similar trends (-7.8 ± 0.9 , $-0.6 \pm 3.4\%$ per decade for ω_1 , ω). The relatively small impact on the post-2002 trend ω , compared to the overall trend-change, is related to O_3 in-mixing from mid-latitudes. Not explicitly accounted for is a possible indirect relationship between ODS-related polar O_3 depletion and tropical LS O_3 by dynamical coupling, as pointed out by several studies (Waugh et al., 2009; Oman et al., 2009). Meul et al. (2014) predict an increase of photolytic O_3 production as a result from long-term changes in the overhead O_3 column. Furthermore, an increase of odd nitrogen (NO_x) might lead to additional O_3 production. However, they found no indication that either process is sufficient to explain a short-term trend-change. Overall the most probable explanation of the observed behaviour is that changes in dynamics must be involved.

3.2 Tropical upwelling

Some studies point out that the increase of tropical upwelling may be compensated by an, as yet, unexplained weakening or shifting of tropical mixing barriers (Stiller et al., 2012; Eckert et al., 2014). However, it is also possible that the increase of tropical upwelling itself has ceased. To investigate this hypothesis, we analyse tropical upwelling in the

EI reanalysis that drives our model. A typical representative quantity for the tropical upwelling is the upward mass flux at 70 hPa (≈ 18.5 km in the tropics; Butchart et al., 2010; Seviour et al., 2012). A recent study assessing the upward mass flux in EI found a negative trend of -5% per decade for the years 1989–2009, based on EI kinematic vertical winds (Seviour et al., 2012). This is in contradiction with the results of current CCMs, which predict an increase of upwelling of about 2.0% per decade (ensemble mean; Butchart et al., 2010). The quality of stratospheric vertical transport in EI improves considerably, when diabatic heating rates are used instead of the kinematic wind. The diabatic representation of vertical transport yields more realistic estimates of stratospheric age of air in comparison to the kinematic approach (Diallo et al., 2012) and is also less dispersive (Ploeger et al., 2011). On the downside, there are indications that EI heating rates overestimate the ascent in the tropics (Ploeger et al., 2012; Diallo et al., 2012). One possible cause for this overestimation could be the usage of a fixed O_3 climatology for calculating the heating rates in the reanalysis (Seviour et al., 2012). Keeping O_3 constant could lead to biased responses to dynamic forcings and thus exaggerating changes in vertical transport. This probably contributes to the differences between model and SAGE II data in the pre-Pinatubo period discussed in Sect. 3.1.

Figure 4 shows the tropical LS EI all-sky heating rates (20°N – 20°S , 17–21 km; panel a), which are used to drive the vertical transport in our isentropic model, and the corresponding EI upward mass flux at 70 hPa (panel c). The upward mass flux is the integral of the residual vertical velocity w^* between turnaround latitudes as described in Seviour et al. (2012). In turn, w^* is calculated from the EI heating rates using the iterative algorithm described by Solomon

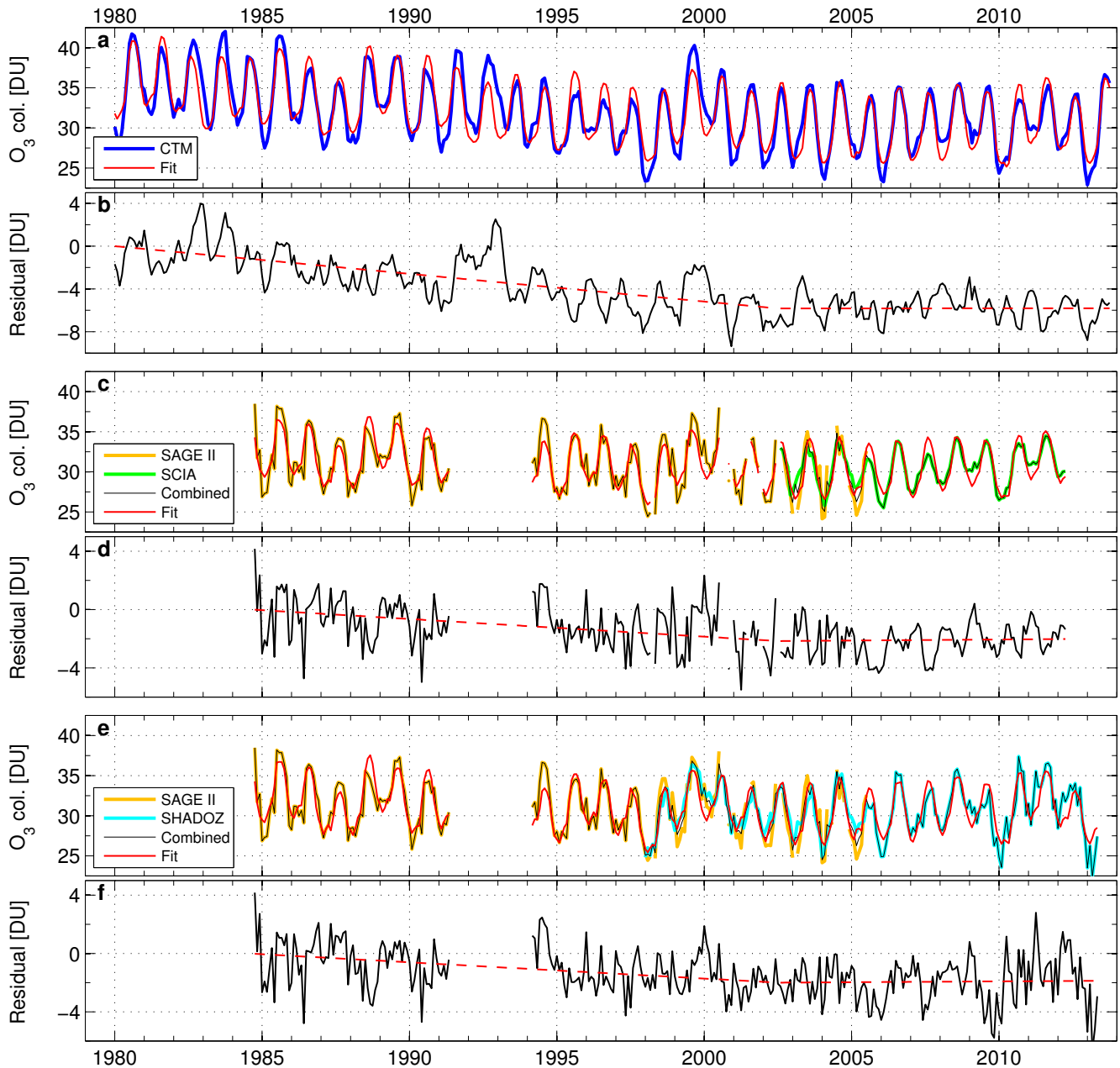


Fig. 3. Regression analysis of observed and simulated O_3 partial columns. Model, combined SAGE II/SCIAMACHY and combined SAGE II/SHADOZ LS O_3 with regression function (a, c, e). Corresponding fit residuals excluding the linear terms (b, d, f). The dashed red lines depict the resulting linear trends before and after 2002.

et al. (1986). Applying the regression analysis to the upward mass flux yields a positive trend of 3.3 ± 0.7 % per decade for the pre-2002 period (ω_1 ; Fig. 4d). This value is consistent with the CCM results (2.0 % per decade) although somewhat high-biased, reflecting the overestimation of vertical transport mentioned above. After 2002, however, there is a statistically significant trend-change around 2002 leading to a negative trend of -2.3 ± 2.5 % per decade (ω) mirroring the

trend-change in the LS O_3 timeseries. Further insight into structural changes of the BDC can be gained by decomposing the circulation into different branches. Here, we adopt the method of Lin and Fu (2013) and define the tropically controlled transition branch, ranging from 100 to 70 hPa and the stratospheric shallow and deep branch (70–30 hPa and <30 hPa, respectively). The strength of the individual branches is estimated by the differences of upward mass fluxes across

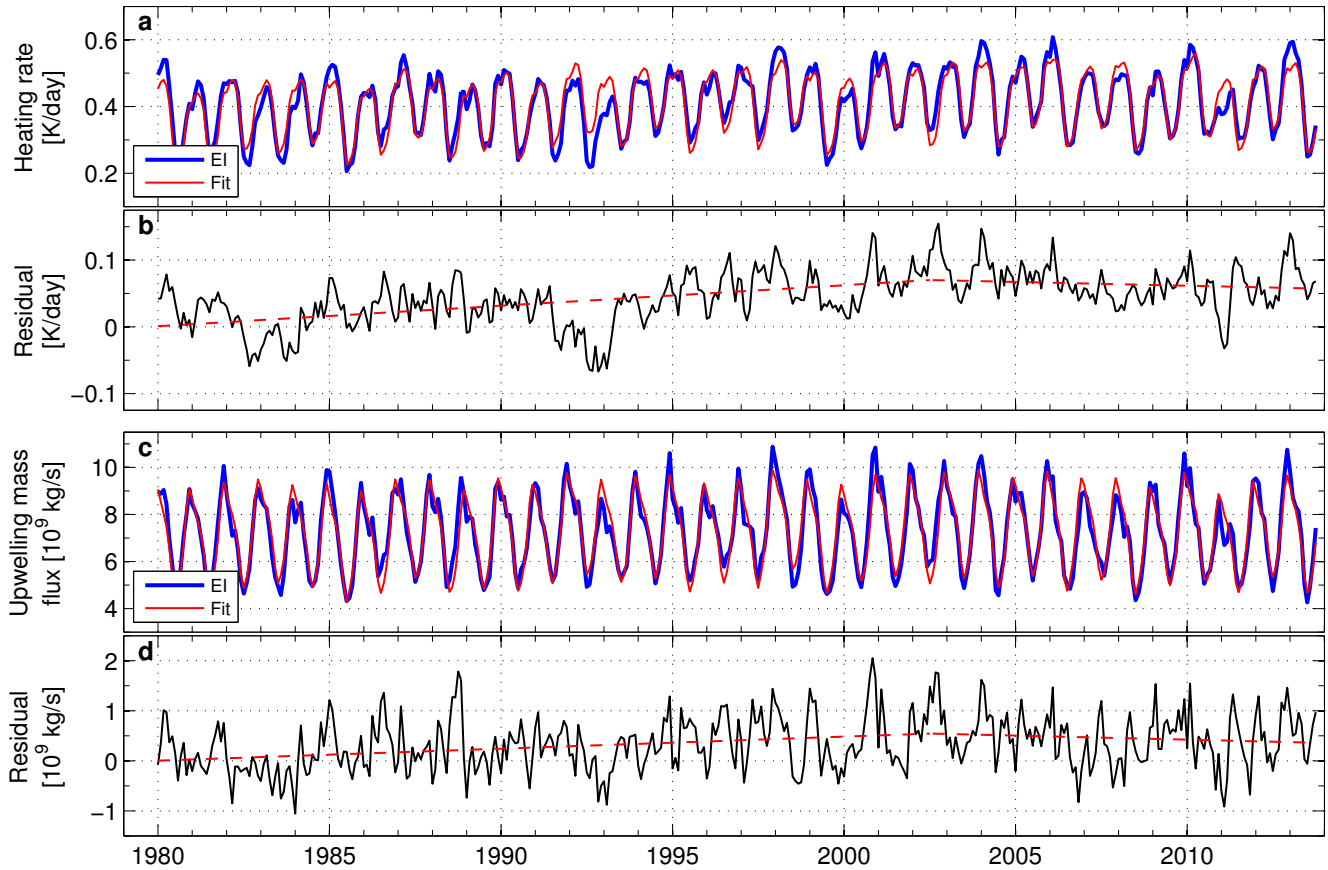


Fig. 4. Regression analysis of EI LS all-sky heating rate (17–21 km; **a**, **b**) and upwelling mass flux (70 hPa; **c**, **d**). Setup identical to Fig. 3 otherwise.

the corresponding boundaries; in case of the deep branch it is simply the flux across the 30 hPa boundary. Figure 5 presents the results of the regression analysis of the mass fluxes in the individual branches, calculated from EI all-sky heating rates as above. In the stratospheric deep branch, there is no significant non-zero trend during the last decades, which is consistent with earlier studies (e.g., Engel et al., 2009; Bönisch et al., 2011; Lin and Fu, 2013). Consequently, the evolution of the shallow branch is dominated by the changes in the 70 hPa flux as discussed above (Fig. 4d), displaying the characteristic trend change around 2002 (5.8 ± 0.9 , -5.6 ± 3.3 % per decade for ω_1 , ω). Interestingly, the transition branch shows the inverted behaviour, a decrease prior to 2002 and an increase afterwards (-9.0 ± 1.1 , 11.1 ± 4.0 % per decade for ω_1 , ω). Apparently there is a shift in mass flux balance from the transition branch towards the shallow branch in earlier decades, which begins to reverse at the beginning of the 21st century. This result does not agree with the findings of Lin and Fu (2013), who calculate positive trends both in the transition and shallow branches based on current CCM simulations. However, Bönisch et al. (2011) detect a significant

increase of the residual circulation around 2000, based on N₂O and O₃ observations. They state that this increase is mainly confined to the lower stratosphere between 100–63 hPa, which is consistent with our definition of the transition branch.

Taking into account the sensitivity of LS O₃ to vertical transport, we conclude that the observed trend-change in O₃ is primarily a consequence of the simultaneous trend-change in tropical upwelling. As the analysed partial columns are dominated by the upper altitudes due to the steep vertical gradient in tropical O₃, they are particularly sensitive to changes in the shallow branch of the BDC between 70–30 hPa. This hypothesis is corroborated by significant anti-correlation between LS O₃ anomalies with either heating rates (-0.83), or 70 hPa upward mass flux anomalies (-0.55).

The cause of these changes is currently unknown. One plausible explanation could be the unexpected La-Niña-like cooling of the equatorial Eastern Pacific since the beginning of the 21st century (Meehl et al., 2011). The latter has a significant impact on global surface temperatures (Kosaka and Xie, 2013) and ultimately, by dynamical coupling, on

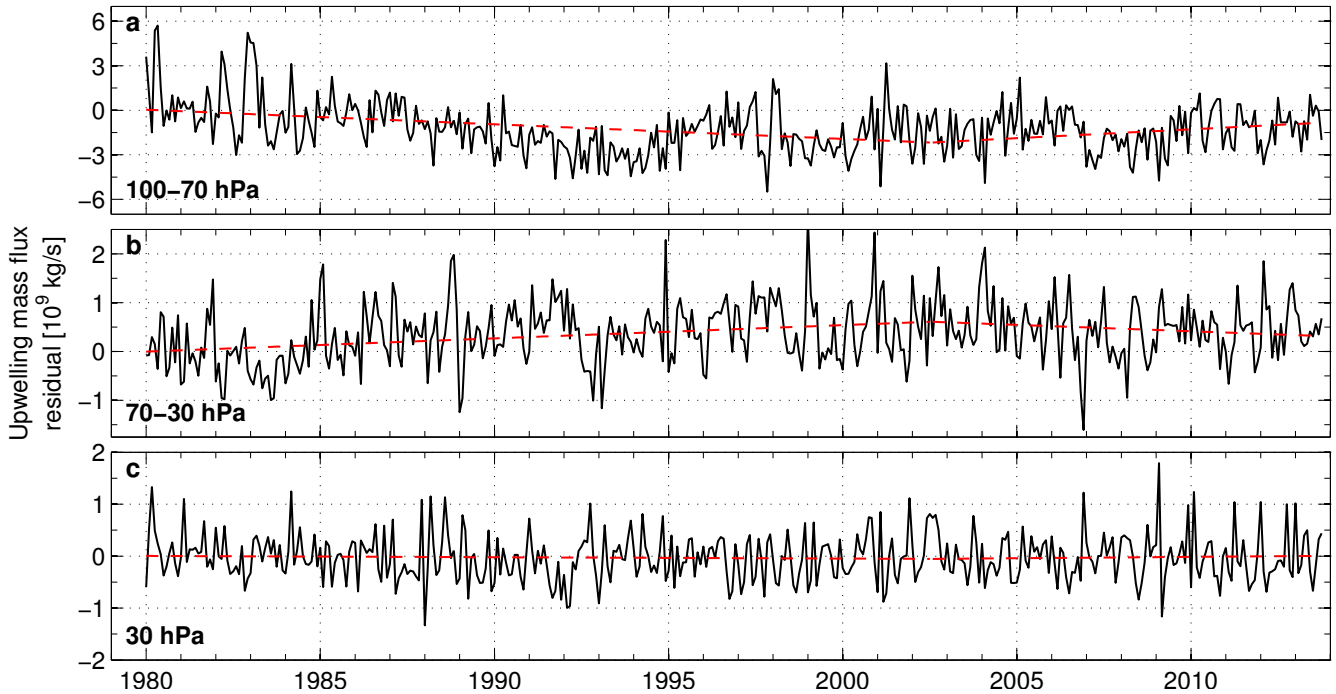


Fig. 5. Fit residuals (excluding linear terms) of EI upwelling mass fluxes in different BDC branches (**a** 100–70 hPa; **b** 70–30 hPa; **c** 30 hPa). The dashed red lines depict the resulting linear trends before and after 2002.

tropical upwelling (Oman et al., 2009; Butchart et al., 2010; Garny et al., 2011). Recent studies describe the associated circulation changes (England et al., 2014) and their impact on tropospheric O_3 (Lin et al., 2014). In contrast to current unconstrained CCM, which generally do not predict this exceptional heat uptake by the equatorial Eastern Pacific (Kosaka and Xie, 2013; England et al., 2014), this feature can be clearly observed in the data-assimilated EI dataset (Fig. 6). This hypothesis is further corroborated by significant (anti-) correlation between tropical surface temperatures and LS upwelling/ O_3 mixing ratios, which is most prominent in the LS (Fig. 7).

4 Conclusions

In this study, we compile observations and model simulations of tropical LS O_3 from 1980–2013. We find negative trends of O_3 both in observation and model before 2002, consistent with earlier studies (e.g., Randel and Thompson, 2011). These trends in O_3 are accompanied by an increase of tropical upwelling found in the EI dataset based upon diabatic heating calculation, confined to the shallow branch of the BDC (70–30 hPa). This is also in agreement with previous modelling studies, which predict an increase of tropical upwelling (e.g., Butchart et al., 2010). However, we also find an unexpected hiatus of the negative trend in LS O_3 after 2002. As we find a similar feature in the behaviour of the vertical

transport in the EI dataset, we conclude that the change in LS O_3 is primarily caused by changes in tropical upwelling. Our analysis shows that the acceleration of the shallow branch has ceased; at the same time the strength of the transition branch (100–70 hPa) increases after about 2002, in agreement with the findings of Bönisch et al. (2011). The deep branch (<30 hPa) does not show any significant changes. Previous modelling studies suggest a dynamical link between tropical SST and upwelling (e.g., Oman et al., 2009). Consequently, it is possible that the detected trend-change in O_3 /upwelling is associated with the recently observed hiatus in tropical SST, caused by an unexpected cooling of the Eastern Pacific (e.g., Meehl et al., 2011). This particular relationship between ocean and atmosphere must be investigated in more detail, as it is likely that the accuracy of our predictions of future BDC development and its consequences for stratospheric O_3 critically depends on our understanding of this interaction.

Acknowledgements. This study has been funded in part by the University and State of Bremen, the DFG Research Unit 1095 Stratospheric Change and its Role for Climate Prediction, SHARP, and the German Federal Ministry of Education and Research, research project Role of the middle atmosphere in climate (ROMIC). SHADOZ, the Southern Hemisphere Additional Ozonesondes network, is funded by NASA's Upper Atmosphere Research Program.

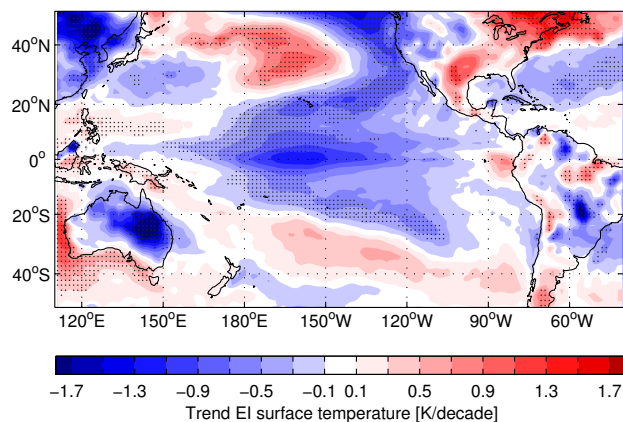


Fig. 6. Linear trends of EI surface temperature from 2002–2013. Stippling indicates where the trend exceeds the 95% confidence threshold. Setup adapted from Kosaka and Xie (2013).

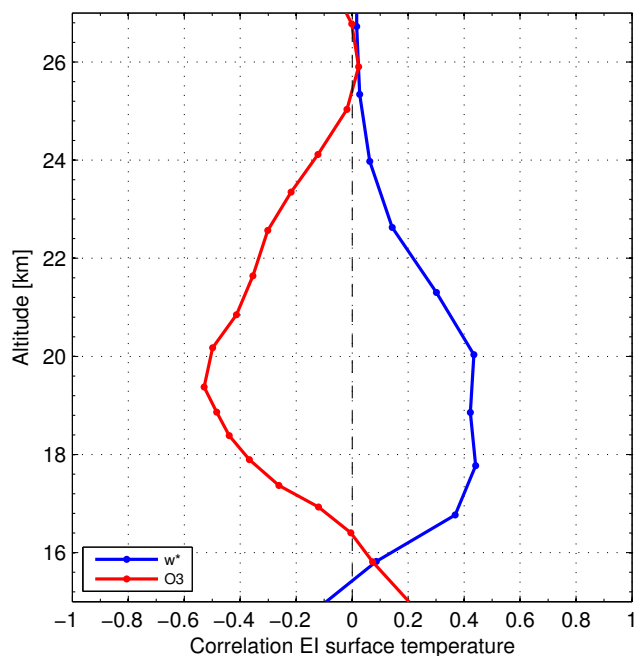


Fig. 7. Correlation of EI surface temperature anomalies with anomalies of w^* calculated from EI all-sky heating rates and modelled O_3 mixing ratios in the tropics ($20^\circ N$ – $20^\circ S$). The corresponding timeseries range from 01-1980 to 10-2013.

References

Abalos, M., Ploeger, F., Konopka, P., Randel, W. J., and Serano, E.: Ozone seasonality above the tropical tropopause: reconciling the Eulerian and Lagrangian perspectives of transport processes, *Atmos. Chem. Phys.*, 13, 10787–10794, doi:

10.5194/acp-13-10787-2013, <http://www.atmos-chem-phys.net/13/10787/2013/>, 2013.

Aschmann, J. and Sinnhuber, B.-M.: Contribution of very short-lived substances to stratospheric bromine loading: uncertainties and constraints, *Atmos. Chem. Phys.*, 13, 1203–1219, doi:10.5194/acp-13-1203-2013, 2013.

Aschmann, J., Sinnhuber, B.-M., Atlas, E. L., and Schauffler, S. M.: Modeling the transport of very short-lived substances into the tropical upper troposphere and lower stratosphere, *Atmos. Chem. Phys.*, 9, 9237–9247, doi:10.5194/acp-9-9237-2009, 2009.

Avallone, L. M. and Prather, M. J.: Photochemical evolution of ozone in the lower tropical stratosphere, *J. Geophys. Res.-Atmos.*, 101, 1457–1461, doi:10.1029/95JD03010, 1996.

Bönisch, H., Engel, A., Birner, T., Hoor, P., Tarasick, D. W., and Ray, E. A.: On the structural changes in the Brewer-Dobson circulation after 2000, *Atmos. Chem. Phys.*, 11, 3937–3948, doi:10.5194/acp-11-3937-2011, 2011.

Bourassa, A. E., Degenstein, D. A., Randel, W. J., Zawodny, J. M., Kyrölä, E., McLinden, C. A., Sioris, C. E., and Roth, C. Z.: Trends in stratospheric ozone derived from merged SAGE II and Odin-OSIRIS satellite observations, *Atmos. Chem. Phys. Discuss.*, 14, 7113–7140, doi:10.5194/acpd-14-7113-2014, <http://www.atmos-chem-phys-discuss.net/14/7113/2014/>, 2014.

Burrows, J., Hölzle, E., Goede, A., Visser, H., and Fricke, W.: SCIAMACHY - scanning imaging absorption spectrometer for atmospheric cartography, *Acta Astronaut.*, 35, 445–451, doi:10.1016/0094-5765(94)00278-T, 1995.

Butchart, N., Cionni, I., Eyring, V., Shepherd, T. G., Waugh, D. W., Akiyoshi, H., Austin, J., Bruehl, C., Chipperfield, M. P., Cordero, E., Dameris, M., Deckert, R., Dhomse, S., Frith, S. M., Garcia, R. R., Gettelman, A., Giorgetta, M. A., Kinnison, D. E., Li, F., Mancini, E., McLandress, C., Pawson, S., Pitari, G., Plummer, D. A., Rozanov, E., Sassi, F., Scinocca, J. F., Shibata, K., Steil, B., and Tian, W.: Chemistry-Climate Model Simulations of Twenty-First Century Stratospheric Climate and Circulation Changes, *J. Clim.*, 23, 5349–5374, doi:10.1175/2010JCLI3404.1, 2010.

Chipperfield, M. P.: Multiannual simulations with a three-dimensional chemical transport model, *J. Geophys. Res.-Atmos.*, 104, 1781–1805, 1999.

Chipperfield, M. P.: New version of the TOMCAT/SOLIMCAT offline chemical transport model: Intercomparison of stratospheric tracer experiments, *Q. J. Roy. Meteor. Soc.*, 132, 1179–1203, doi:10.1256/qj.05.51, 2006.

Damadeo, R. P., Zawodny, J. M., Thomason, L. W., and Iyer, N.: SAGE version 7.0 algorithm: application to SAGE II, *Atmos. Meas. Tech.*, 6, 3539–3561, doi:10.5194/amt-6-3539-2013, 2013.

Dee, D. P., Uppala, S. M., Simmons, A. J., Berrisford, P., Poli, P., Kobayashi, S., Andrae, U., Balmaseda, M. A., Balsamo, G., Bauer, P., Bechtold, P., Beljaars, A. C. M., van de Berg, L., Bidlot, J., Bormann, N., Delsol, C., Dragani, R., Fuentes, M., Geer, A. J., Haimberger, L., Healy, S. B., Hersbach, H., Hólm, E. V., Isaksen, L., Kållberg, P., Köhler, M., Matricardi, M., McNally, A. P., Monge-Sanz, B. M., Morcrette, J.-J., Park, B.-K., Peubey, C., de Rosnay, P., Tavolato, C., Thépaut, J.-N., and Vitart, F.: The ERA-Interim reanalysis: configuration and performance of the data assimilation system, *Q. J. Roy. Meteor. Soc.*, 137, 553–597, doi:10.1002/qj.828, 2011.

- Diallo, M., Legras, B., and Chédin, A.: Age of stratospheric air in the ERA-Interim, *Atmos. Chem. Phys.*, 12, 12 133–12 154, doi:10.5194/acp-12-12133-2012, 2012.
- Eckert, E., von Clarmann, T., Kiefer, M., Stiller, G. P., Lossow, S., Glatthor, N., Degenstein, D. A., Froidevaux, L., Godin-Beekmann, S., Leblanc, T., McDermid, S., Pastel, M., Steinbrecht, W., Swart, D. P. J., Walker, K. A., and Bernath, P. F.: Drift-corrected trends and periodic variations in MIPAS IMK/IAA ozone measurements, *Atmos. Chem. Phys.*, 14, 2571–2589, doi:10.5194/acp-14-2571-2014, <http://www.atmos-chem-phys.net/14/2571/2014/>, 2014.
- Engel, A., Moebius, T., Bönisch, H., Schmidt, U., Heinz, R., Levin, I., Atlas, E., Aoki, S., Nakazawa, T., Sugawara, S., Moore, F., Hurst, D., Elkins, J., Schauffler, S., Andrews, A., and Boering, K.: Age of stratospheric air unchanged within uncertainties over the past 30 years, *Nat. Geosci.*, 2, 28–31, doi:10.1038/NNGEO388, 2009.
- England, M. H., McGregor, S., Spence, P., Meehl, G. A., Timmermann, A., Cai, W., Gupta, A. S., McPhaden, M. J., Purich, A., and Santoso, A.: Recent intensification of wind-driven circulation in the Pacific and the ongoing warming hiatus, *Nat. Clim. Change*, 4, 222–227, doi:10.1038/nclimate2106, 2014.
- García, R. R. and Randel, W. J.: Acceleration of the Brewer-Dobson circulation due to increases in greenhouse gases, *J. Atmos. Sci.*, 65, 2731–2739, doi:10.1175/2008JAS2712.1, 2008.
- Garny, H., Dameris, M., Randel, W., Bodeker, G. E., and Deckert, R.: Dynamically Forced Increase of Tropical Upwelling in the Lower Stratosphere, *J. Atmos. Sci.*, 68, 1214–1233, doi:10.1175/2011JAS3701.1, 2011.
- Gebhardt, C., Rozanov, A., Hommel, R., Weber, M., Bovensmann, H., Burrows, J. P., Degenstein, D., Froidevaux, L., and Thompson, A. M.: Stratospheric ozone trends and variability as seen by SCIAMACHY from 2002 to 2012, *Atmos. Chem. Phys.*, 14, 831–846, doi:10.5194/acp-14-831-2014, <http://www.atmos-chem-phys.net/14/831/2014/>, 2014.
- Jones, A., Urban, J., Murtagh, D. P., Eriksson, P., Brohede, S., Haley, C., Degenstein, D., Bourassa, A., von Savigny, C., Sonkaew, T., Rozanov, A., Bovensmann, H., and Burrows, J.: Evolution of stratospheric ozone and water vapour time series studied with satellite measurements, *J. Atmos. Sci.*, 9, 6055–6075, doi:10.5194/acp-9-6055-2009, 2009.
- Kawatani, Y. and Hamilton, K.: Weakened stratospheric quasibiennial oscillation driven by increased tropical mean upwelling, *Nature*, 497, 478–481, doi:10.1038/nature12140, 2013.
- Konopka, P., Grooss, J.-U., Ploeger, F., and Mueller, R.: Annual cycle of horizontal in-mixing into the lower tropical stratosphere, *J. Geophys. Res.-Atmos.*, 114, doi:10.1029/2009JD011955, 2009.
- Kosaka, Y. and Xie, S.-P.: Recent global-warming hiatus tied to equatorial Pacific surface cooling, *Nature*, 501, 403–407, doi:10.1038/nature12534, 2013.
- Kyrölä, E., Laine, M., Sofieva, V., Tamminen, J., Päivärinta, S.-M., Tukiainen, S., Zawodny, J., and Thomason, L.: Combined SAGE IIGOMOS ozone profile data set for 1984–2011 and trend analysis of the vertical distribution of ozone, *Atmos. Chem. Phys.*, 13, 10 645–10 658, doi:10.5194/acp-13-10645-2013, <http://www.atmos-chem-phys.net/13/10645/2013/>, 2013.
- Lin, M., Horowitz, L. W., Oltmans, S. J., Fiore, A. M., and Fan, S.: Tropospheric ozone trends at Mauna Loa Observatory tied to decadal climate variability, *Nat. Geosci.*, 7, 136–143, doi:10.1038/ngeo2066, 2014.
- Lin, P. and Fu, Q.: Changes in various branches of the Brewer-Dobson circulation from an ensemble of chemistry climate models, *J. Geophys. Res.-Atmos.*, 118, 73–84, doi:10.1029/2012JD018813, 2013.
- McCormick, M., Zawodny, J., Veiga, R., Larsen, J., and Wang, P.: An overview of SAGE-I and SAGE-II ozone measurements, *Planet. Space Sci.*, 37, 1567–1586, doi:10.1016/0032-0633(89)90146-3, 1989.
- Meehl, G. A., Arblaster, J. M., Fasullo, J. T., Hu, A., and Trenberth, K. E.: Model-based evidence of deep-ocean heat uptake during surface-temperature hiatus periods, *Nat. Clim. Change*, 1, 360–364, doi:10.1038/NCLIMATE1229, 2011.
- Meul, S., Langematz, U., Oberländer, S., Garny, H., and Jöckel, P.: Chemical contribution to future tropical ozone change in the lower stratosphere, *Atmos. Chem. Phys.*, 14, 2959–2971, doi:10.5194/acp-14-2959-2014, <http://www.atmos-chem-phys.net/14/2959/2014/>, 2014.
- Oman, L., Waugh, D. W., Pawson, S., Stolarski, R. S., and Newman, P. A.: On the influence of anthropogenic forcings on changes in the stratospheric mean age, *J. Geophys. Res.-Atmos.*, 114, doi:10.1029/2008JD010378, 2009.
- Ploeger, F., Fueglistaler, S., Grooss, J. U., Guenther, G., Konopka, P., Liu, Y. S., Mueller, R., Ravegnani, F., Schiller, C., Ulanovski, A., and Riese, M.: Insight from ozone and water vapour on transport in the tropical tropopause layer (TTL), *Atmos. Chem. Phys.*, 11, 407–419, doi:10.5194/acp-11-407-2011, 2011.
- Ploeger, F., Konopka, P., Mueller, R., Fueglistaler, S., Schmidt, T., Manners, J. C., Grooss, J.-U., Guenther, G., Forster, P. M., and Riese, M.: Horizontal transport affecting trace gas seasonality in the Tropical Tropopause Layer (TTL), *J. Geophys. Res.-Atmos.*, 117, doi:10.1029/2011JD017267, 2012.
- Polvani, L. M. and Solomon, S.: The signature of ozone depletion on tropical temperature trends, as revealed by their seasonal cycle in model integrations with single forcings, *J. Geophys. Res.-Atmos.*, 117, doi:10.1029/2012JD017719, 2012.
- Randel, W. J. and Jensen, E. J.: Physical processes in the tropical tropopause layer and their roles in a changing climate, *Nat. Geosci.*, 6, 169–176, doi:10.1038/ngeo1733, 2013.
- Randel, W. J. and Thompson, A. M.: Interannual variability and trends in tropical ozone derived from SAGE II satellite data and SHADOZ ozonesondes, *J. Geophys. Res.-Atmos.*, 116, doi:10.1029/2010JD015195, 2011.
- Randel, W. J., Wu, F., Voemel, H., Nedoluha, G. E., and Forster, P.: Decreases in stratospheric water vapor after 2001: Links to changes in the tropical tropopause and the Brewer-Dobson circulation, *J. Geophys. Res.-Atmos.*, 111, doi:10.1029/2005JD006744, 2006.
- Reinsel, G. C., Weatherhead, E. C., Tiao, G. C., Miller, A. J., Nagatani, R. M., Wuebbles, D. J., and Flynn, L. E.: On detection of turnaround and recovery in trend for ozone, *J. Geophys. Res.-Atmos.*, 107, doi:10.1029/2001JD000500, 2002.
- Sander, S. P. et al.: Chemical Kinetics and Photochemical Data for Use in Atmospheric Studies: Evaluation No. 17, JPL Publ. 10-6, Jet Propul. Lab., Pasadena, CA, 2011.
- Seviour, W. J. M., Butchart, N., and Hardiman, S. C.: The Brewer-Dobson circulation inferred from ERA-Interim, *Q. J. Roy. Meteor. Soc.*, 138, 878–888, doi:10.1002/qj.966, 2012.
- Sinnhuber, B.-M., Weber, M., Amankwah, A., and Burrows, J. P.:

- Total ozone during the unusual Antarctic winter of 2002, *Geophys. Res. Lett.*, 30, doi:10.1029/2002GL016798, 2003.
- Sioris, C. E., McLinden, C. A., Fioletov, V. E., Adams, C., Zawodny, J. M., Bourassa, A. E., Roth, C. Z., and Degenstein, D. A.: Trend and variability in ozone in the tropical lower stratosphere over 2.5 solar cycles observed by SAGE II and OSIRIS, *Atmos. Chem. Phys.*, 14, 3479–3496, doi:10.5194/acp-14-3479-2014, <http://www.atmos-chem-phys.net/14/3479/2014/>, 2014.
- Snow, M., Weber, M., Machol, J., Viereck, R., and Richard, E.: Comparison of Magnesium II core-to-wing ratio observations during solar minimum 23/24, *J. Space Weather Space Clim.*, 4, A04, doi:10.1051/swsc/2014001, 2014.
- Solomon, S., Kiehl, J. T., Garcia, R. R., and Grose, W.: Tracer transport by the diabatic circulation deduced from satellite-observations, *J. Atmos. Sci.*, 43, 1603–1617, doi:10.1175/1520-0469(1986)043<1603:TTBTDC>2.0.CO;2, 1986.
- Sonkaew, T., Rozanov, V. V., von Savigny, C., Rozanov, A., Bovensmann, H., and Burrows, J. P.: Cloud sensitivity studies for stratospheric and lower mesospheric ozone profile retrievals from measurements of limb-scattered solar radiation, *Atmos. Meas. Tech.*, 2, 653–678, 2009.
- Stiller, G. P., von Clarmann, T., Haenel, F., Funke, B., Glatthor, N., Grabowski, U., Kellmann, S., Kiefer, M., Linden, A., Lossow, S., and López-Puertas, M.: Observed temporal evolution of global mean age of stratospheric air for the 2002 to 2010 period, *Atmos. Chem. Phys.*, 12, 3311–3331, doi:10.5194/acp-12-3311-2012, 2012.
- Thompson, A. M., Witte, J. C., McPeters, R. D., Oltmans, S. J., Schmidlin, F. J., Logan, J. A., Fujiwara, M., Kirchhoff, V. W. J. H., Posny, F., Coetzee, G. J. R., Hoegger, B., Kawakami, S., Ogawa, T., Johnson, B. J., Vömel, H., and Labow, G.: Southern Hemisphere Additional Ozonesondes (SHADOZ) 1998-2000 tropical ozone climatology - 1. Comparison with Total Ozone Mapping Spectrometer (TOMS) and ground-based measurements, *J. Geophys. Res.-Atmos.*, 108, doi:10.1029/2001JD000967, 2003.
- Thompson, A. M., Miller, S. K., Tilmes, S., Kollonige, D. W., Witte, J. C., Oltmans, S. J., Johnson, B. J., Fujiwara, M., Schmidlin, F. J., Coetzee, G. J. R., Komala, N., Maata, M., Mohamad, M. B., Nguyo, J., Mutai, C., Ogino, S.-Y., Da Silva, F. R., Paes Leme, N. M., Posny, F., Scheele, R., Selkirk, H. B., Shiotani, M., Stuebi, R., Levrat, G., Calpini, B., Thouret, V., Tsuruta, H., Valverde Canossa, J., Voemel, H., Yonemura, S., Andres Diaz, J., Thanh, N. T. T., and Ha, H. T. T.: Southern Hemisphere Additional Ozonesondes (SHADOZ) ozone climatology (2005-2009): Tropospheric and tropical tropopause layer (TTL) profiles with comparisons to OMI-based ozone products, *J. Geophys. Res.-Atmos.*, 117, doi:10.1029/2011JD016911, 2012.
- Thompson, D. and Solomon, S.: Recent stratospheric climate trends as evidenced in radiosonde data: Global structure and tropospheric linkages, *J. Climate*, 18, 4785–4795, doi:10.1175/JCLI3585.1, 2005.
- Wang, H., Cunnold, D., Thomason, L., Zawodny, J., and Bodeker, G.: Assessment of SAGE version 6.1 ozone data quality, *J. Geophys. Res.-Atmos.*, 107, doi:10.1029/2002JD002418, 2002.
- Waugh, D. W., Oman, L., Kawa, S. R., Stolarski, R. S., Pawson, S., Douglass, A. R., Newman, P. A., and Nielsen, J. E.: Impacts of climate change on stratospheric ozone recovery, *Geophys. Res. Lett.*, 36, doi:10.1029/2008GL036223, 2009.
- Wolter, K. and Timlin, M. S.: El Nino/Southern Oscillation behaviour since 1871 as diagnosed in an extended multivariate ENSO index (MEI.ext), *Int. J. Climatol.*, 31, 1074–1087, doi:10.1002/joc.2336, 2011.
- World Meteorological Organization: Scientific Assessment of Ozone Depletion: 2010, Global Ozone Research and Monitoring Project-Report No. 52, Geneva, Switzerland, 2011.
- Young, P. J., Rosenlof, K. H., Solomon, S., Sherwood, S. C., Fu, Q., and Lamarque, J.-F.: Changes in Stratospheric Temperatures and Their Implications for Changes in the Brewer Dobson Circulation, 1979-2005, *J. Climate*, 25, 1759–1772, doi:10.1175/2011JCLI4048.1, 2012.